DETAILED STUDIES OF MANGANESE IN SILICON USING LIFETIME SPECTROSCOPY AND DEEP-LEVEL TRANSIENT SPECTROSCOPY

P. Rosenits[1], T. Roth[1], S. Diez[1,†], D. Macdonald[2], S.W. Glunz[1]

[1]Fraunhofer Institute for Solar Energy Systems (ISE), Heidenhofstrasse 2, D-79110 Freiburg, Germany
[2]Department of Engineering, FEIT, Australian National University (ANU), Canberra, 0200 ACT, Australia
[†]Now with Q-Cells AG, Guardianstrasse 16, D-06766 Thalheim, Germany
Phone: +49 761 4588 5366, Fax: +49 761 4588 9250, Email: philipp.rosenits@ise.fraunhofer.de

ABSTRACT: Different characterisation methods, particularly injection-dependent lifetime spectroscopy (IDLS), deep-level transient spectroscopy (DLTS) and temperature-dependent lifetime spectroscopy (TDLS), have been applied to investigate the defect parameters of manganese in silicon. The results of the two latter methods are presented in this paper. Special interest lay in the study of the manganese-boron pairs which could be detected by means of DLTS at low temperatures in the samples. They have been dissociated optically and thermally and subsequently analysed with lifetime spectroscopy. Furthermore the recombination-dominating defect level of interstitial manganese in silicon could be determined for the first time.
Keywords: Manganese, Defects, Lifetime

1 INTRODUCTION

In the past decades, growing efforts have been dedicated to identify and investigate the properties of 3*d* transition metal impurities in silicon. A precise determination of their energy levels and capture cross sections as well as a profound understanding of any pairing behaviour with other impurity or doping atoms is of both enormous theoretical and technological interest.
Manganese is one of the transition metals and is located in the periodic table in between chromium and iron. Like Fe and Cr, it has a moderately high solid solubility limit at typical device processing temperatures, as well as a relatively high diffusivity. This makes it a potentially dangerous impurity during the processing of devices such as solar cells, as it may introduce high concentrations of distributed point-like recombination centres.

In comparison to the vast number of investigations and publications about iron and its complexes in silicon (see for example [1]), relatively few is reported about manganese to the present. The aim of the work presented here is to characterise a set of Mn-contaminated samples by different characterisation methods, particularly deep-level transient spectroscopy (DLTS) [2] and temperature-dependent lifetime spectroscopy (TDLS) [3], and critically assess if the results for the defect parameters agree with each other as well as with literature.

2 ELECTRONIC PROPERTIES OF MANGANESE IN SILICON

Manganese forms part of the 3*d* transition metals and is located between chromium and iron in the periodic table. The only naturally occurring isotope is ^{55}Mn, with an atomic mass of $m_a = 54.94u$ ($u = 1.6605\times10^{-27}$ kg) and a nuclear charge of 25*e*, *e* signifying the elementary charge. The solubility and diffusivity of manganese atoms within the silicon crystal lattice is relatively high and quite similar to iron [4] in the temperature range of 300 to 1500 K that is relevant for most silicon device processing steps, e.g. solar cell processing.

If impurity atoms are introduced into the silicon crystal, they can in general take up interstitial or substitutional places, as well as forming pairs, clusters or precipitates with each other or different atoms that are present in the crystal. It was discovered very early that manganese exists in silicon in a stable form interstitially (Mn_i) as well as substitutionally (Mn_s) [5, 6]. In addition it is known that manganese forms donor-acceptor-pairs with boron, aluminium, gallium, tin and gold [4]. Pairing with further metals has not been observed yet, but cannot be excluded either. A particularity of manganese is the formation of Mn_4 clusters consisting of four interstitial Mn atoms [4].

The structure, charge states and energy levels of Mn-related centres in silicon have been investigated in several studies since the 1950s. The energy levels and majority capture cross sections of interstitial manganese are quite well-established and the number of works thereto satisfactorily summarised by Graff [4] who presents a weighted average for the defect parameters (see Table II). As can be seen, Mn_i occurs in four different charge states, leading to three energy levels in the band gap, an acceptor at E_C – 0.12 eV, a donor at E_C – 0.43 eV and a double donor at E_V + 0.27 eV.

For the second defect configuration of manganese, namely the manganese-boron-pairs, publications concerning its defect parameters are less numerous [7-10] and listed in Table I. These investigations agree that MnB introduces one single deep donor level in the silicon band gap, with values ranging from E_C – 0.50 to E_C – 0.57 eV.

Finally, there are a few quantitative studies about the defect parameters of substitutional manganese in silicon [8, 11-13], indicating that Mn_s exists in three charge states, leading to an acceptor in the upper band gap half and a donor level in the lower band gap half.

In summary it can be said that manganese shows a far more complex defect structure than iron or chromium for instance, that normally do not exist in substitutional form and also only exhibit one single interstitial energy level in the silicon band gap. A consequence of these additional energy levels for Mn is that it is difficult to state *a priori* which level dominates recombination, as the populations of the various charge states will depend on the Fermi level, i.e. on doping type and concentration. Under strong charge carrier injection, the quasi-Fermi levels influence the occupation of the different charge

states as well, which means that the dominating recombination level can also change depending on the injection density.

3 SAMPLE PREPARATION

The sample preparation has been described in detail in [14] where first results from lifetime measurements on the Mn-implanted samples have been presented. Therefore, in this report only the most important facts regarding sample preparation should be summarised and otherwise referred to the above mentioned literature.

The silicon wafers used in this study were float-zone grown with a surface orientation of <100>. The samples were boron-doped with resistivities of either 1 Ωcm ($N_A = 1.5\times10^{16}$ cm^{-3}, 460 µm thick), 20 Ωcm ($N_A = 6.8\times10^{14}$ cm^{-3}, 500 µm thick) or 40 Ωcm ($N_A = 3.4\times10^{14}$ cm^{-3}, 200 µm thick).

After standard cleaning samples of each resistivity were implanted with MnO^- ions at an energy of 70 keV to a dose of 5×10^{11} cm^{-2}. Following further surface cleaning and native oxide removal, the samples were then annealed at 900°C for 100 min to distribute the implanted Mn throughout the samples, followed by rapid cooling in air to room temperature. Interstitial manganese has a diffusivity of approximately 1.5×10^{-6} cm^2 s^{-1} at $T = 900$°C [4], resulting in a diffusion length of 930 µm for these annealing conditions, significantly greater than the wafer thickness. In the absence of precipitation, this should result in an approximately uniform distribution of Mn throughout the thickness of the wafers.

Note that the low energy and dose used here do not result in any residual lifetime-reducing crystal damage as this has been previously shown to be effectively removed during such annealing [15]. In addition, it was necessary to implant MnO^- ions due to the very low yield of Mn ions. It is assumed that the MnO molecules break up upon implantation. This results in separated Mn and O atoms in the thin implanted sub-surface region, which are then distributed throughout the wafer thickness by the annealing. Considering that the average oxygen concentration after annealing corresponding to the doses used here is much less than the natural oxygen concentration in this material, the implanted O atoms are not expected to significantly affect the subsequent lifetime measurements [16].

4 RESULTS AND DISCUSSION

To characterise the manganese-implanted samples, different characterisation methods have been applied: IDLS using the quasi-steady-state photoconductance (QSSPC) method [17], DLTS as well as TDLS using a microwave-detected photoconductance decay setup (MW-PCD). While the results of the QSSPC measurements have already been presented recently [14], this paper will focus on the DLTS and TDLS investigations.

4.1 DLTS measurements

In order to prepare the samples for the DLTS investigations, Schottky and ohmic contacts have been applied on both sides of the wafers. After standard HF etching the contacts were sputtered onto the silicon wafers in a sputtering chamber at 2×10^{-6} mbar and temperatures not above 55°C. To achieve a Schottky contact on *p*-type material, 30 nm titanium and 60 nm aluminium have been deposited on one side of the samples through a mask allowing distinct circular contact areas with diameters ranging from 0.2 to 1 mm. The requirement of an ohmic contact on the other side was met with covering the back side of the wafer entirely with a 60 nm aluminium layer. The measurements were carried out using a digital DLTS system FT1030 from PhysTech. Fourier based weighting functions were used to calculate the DLTS spectrum from the measured capacity transients.

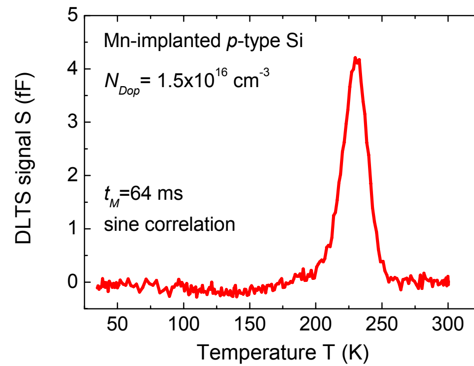

Figure 1: DLTS spectrum of the 1 Ωcm boron-doped FZ silicon sample that was implanted with manganese.

The DLTS signal for a given correlation function (sine correlation) is depicted in Fig. 1. As can be seen, the signal-noise ratio is satisfying, which is mainly due to a relatively high defect concentration of $N_t = 2\times10^{-3} N_A$. The peak around 230 K was evaluated for every rate window and in Fig. 2 the resulting Arrhenius plot of the different DLTS spectra (for different rate windows) is shown. From these data, an energy depth of $E_t - E_V = 0.56 \pm 0.03$ eV, a majority carrier capture cross section of $\sigma_p = 5.2\times10^{-13}$ cm^2 (at $T = 230$ K) and a defect density of $N_t = 3.5\times10^{13}$ cm^{-3} could be extracted. As usual for DLTS measurements, the value for the capture cross section has to be treated with precaution, since this value is obtained by the extrapolation of the Arrhenius fit to infinite temperatures. Note that any additional contamination with iron during sample preparation would have led to a DLTS peak around 50 K, being related to iron-boron pairs with an energy level of $E_V + 0.10$ eV [1]. However, only one peak at around 230 K was observed.

A similar DLTS analysis has been performed for the Mn-contaminated sample having a resistivity of 40 Ωcm, yielding an energy depth of $E_t - E_V = 0.53 \pm 0.03$ eV, a majority carrier capture cross section of $\sigma_p = 1.8\times10^{-13}$ cm^2 and a defect density of $N_t = 8.2\times10^{11}$ cm^{-3}. This measured defect concentration is more than one order of magnitude lower than the expected concentration calculated from the implantation dose. It is not yet resolved if there occurred a problem during the implantation, precipitation during annealing, or during DLTS measurements. However, the energy depth and also the capture cross sections agree fairly well between the two measurements, implying reliable DLTS measurements and analysis.

Comparing theses values with published data for Mn-related defects from the literature (see Table I for details), we were able to identify the detected impurity level with the defect level of manganese-boron pairs, which are obviously present within the sample at the temperatures used for the DLTS measurement, namely below room temperature .

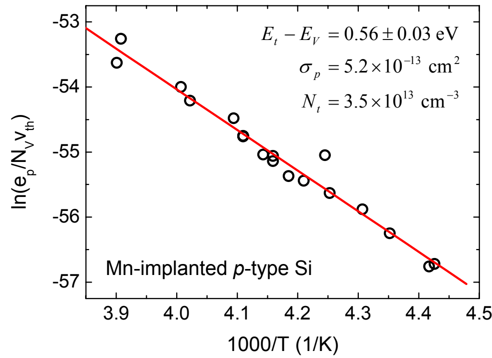

Figure 2: Arrhenius plot of the 1 Ωcm Mn-implanted sample. In the insert the extracted defect parameters, i.e. energy level, hole capture cross section and defect concentration, are shown.

4.2 Temperature-dependent lifetime spectroscopy

In the following, parts of the wafers have been prepared for lifetime measurements. To minimise the effect of surface recombination on the effective charge carrier lifetime, the lifetime samples have been passivated by a 70 nm silicon-nitride (SiN) layer, deposited via plasma-enhanced chemical vapour deposition (PECVD) during 10 min at 350°C on both sides of the wafer.

The DLTS measurements were only possible to be carried out in the dark and at temperatures below room temperature. For this reason only the defect parameters of the manganese-boron pairs could be determined. In order to access the defect parameters of the dissociated MnB pairs, i.e. interstitial manganese, the intention of the lifetime measurements was therefore to take advantage of the facilities of the microwave-detected photoconductance decay (MW-PCD) setup at Fraunhofer ISE where the samples can be illuminated up to 0.3 W/cm^2 and a cryostatic device allows measurements in a temperature range from 77 to 600 K.

Consequently, the effective charge carrier lifetimes at low level injection were measured over the whole temperature range once in the dark (only very weak bias light was allowed during measurements to exclude distortions due to trapping) and once the Mn-implanted samples being illuminated continuously with white light of approximately 0.3 W/cm^2 (with the only exception of the very short time periods of the actual lifetime measurement procedure where the illumination had to be switched off). As the complete measuring of one sample took in general several days and the sample was exposed to very different temperatures, some temperature ranges were measured repeatedly to ensure that the defect configuration did not change in the mean time which was indeed the case.

Fig. 3 shows the resulting graph of the temperature normalised low-level injection lifetime in the dark (black, open circles) and under illumination (red, closed circles). It exhibits four interesting temperature regions: While the low-level injection lifetime below a temperature of approximately –50°C is only affected by the temperature-dependent minority carrier cross section, in the temperature range from –40°C to +140°C the different lifetimes related to two different defect configurations under the two varying illumination conditions are clearly visible. Above a temperature of +160°C, a linear Arrhenius increase can be observed. Intrinsic conduction is finally starting to dominate the effective lifetime at around +250°C.

In order to extract the defect parameters of the Mn-related defect configuration at higher temperatures, a TDLS fit has been performed for the illuminated curve. Minimising the least square fit error χ^2, two parameter sets with nearly the same fit quality were obtained, one in the upper band gap half at $E_C - E_t$ = 0.46 eV having a symmetry factor $k := \sigma_n/\sigma_p$ = 9.4 and another one in the lower band gap half at $E_t - E_V$ = 0.37 eV with k = 23.1. Comparing these two possible numerical solutions with reported data from the literature for manganese-related defects, we were able to relate the first solution to interstitial manganese ($E_C - E_t$ = 0.46 eV). The k-factor has been determined for the first time to the authors' knowledge.

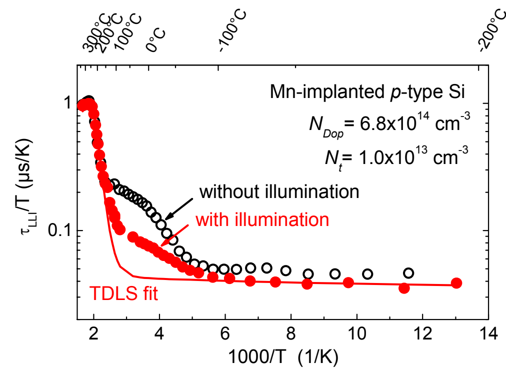

Figure 3: Temperature-dependent lifetime spectroscopy of a 20 Ωcm manganese-implanted sample. The low level injection carrier lifetime has been measured once in the dark and once under 0.3 W/cm^2 illumination. The partial optical dissociation of the MnB pairs in the temperature range between 200 and 400 K is clearly visible due to the different lifetimes. The solid line represents a TDLS fit to the illuminated data with the parameters $E_C - E_t$ = 0.46 ± 0.04 eV and k = 9 ± 7.

4.3 Discussion

A weighted average of the defect parameters for the defect centre introduced by the implantation of MnO^- ions could be obtained via DLTS measurements on the 1 Ωcm and 40 Ωcm samples and resulted in $E_t - E_V$ = 0.54 ± 0.02 eV and σ_p = 3.5×10^{-13} cm^2. A comparison with previous publications about defect levels of Mn in Si confirmed the assumption that the implanted manganese atoms formed pairs with the boron dopants after implantation. Table I gives a detailed overview of previous works on the determination of the defect parameters of MnB pairs. The values found in this study agree very well with the results of Lemke, Nakashima and Carlson. The hole capture cross section was determined for the first time in this work.

Table I: Overview of all previous publications regarding the defect parameters of the manganese-boron pairs in silicon as well as results from this work (bold). All values have been obtained using deep-level transient spectroscopy.

Investigated defect: **Manganese-Boron Pairs (MnB)**		
Reference/ Sample ID	Defect Energy Level ΔE_t (eV)	Capture Cross Section σ (cm^2)
Lemke [9]	$E_C - 0.55$	$\sigma_n = 9\times10^{-14}$
Lemke [10]	$E_C - 0.57$	
Nakashima [8]	$E_C - 0.50$	
Carlson [7]	$E_C - 0.53$	
this work (Mn_1P)	$\mathbf{(E_V + 0.56) \pm 0.03}$	$\mathbf{\sigma_p = 5.2\times10^{-13}}$
this work (Mn_40P)	$\mathbf{(E_V + 0.53) \pm 0.03}$	$\mathbf{\sigma_p = 1.8\times10^{-13}}$

Table II: Overview of the defect parameters of interstitial manganese in silicon, comprising data from literature as well as results from this work (bold).

Investigated defect: **Interstitial Manganese (Mn_i)**			
Reference/ Sample ID	Defect Energy Level ΔE_t (eV)	Capture Cross Section σ (cm^2)	Measurement Method
Graff [4]	$E_C - 0.12$	σ_n =3.1×10^{-15}	DLTS
	$E_C - 0.43$	σ_n =3.1×10^{-15}	DLTS
	$E_V + 0.27$	σ_p =2.0×10^{-18}	DLTS
this work (Mn_20P)	$\mathbf{(E_C - 0.46) \pm 0.04}$	$\mathbf{\sigma_n = (9 \pm 7)\sigma_p}$	**TDLS**

Subsequently, these manganese-boron pairs have been investigated more closely using MW-PCD. Fig. 3 shows that the MnB pairs can indeed be dissociated thermally and optically. The lifetime curves are to be interpreted in the following way: For temperatures $T < 200$ K all manganese atoms are paired with the boron dopants. In a relatively large transition region at 200 K < $T < 400$ K they dissociate increasingly and eventually only exist in interstitial form for temperatures $T > 400$ K. By means of a constant illumination of 0.3 W/cm^2 MnB pairs can also get dissociated for $T < 400$ K what has been done for the first time in the present work. However, the difference between the illuminated carrier lifetime curve and the fitted TDLS curve, that represents the lifetime if exclusively interstitial manganese existed, suggest that a considerable fraction, though not all, MnB pairs have been dissociated optically.

Via the TDLS fit the defect parameters of interstitial manganese could be determined to $E_C - E_t = 0.46 \pm 0.04$ eV and $\sigma_n = (9 \pm 7)\sigma_p$ which agrees well with the values presented by Graff [4]. The progress in the understanding and characterisation of manganese in silicon achieved by this work is the knowledge which one of the three defect levels that is introduced by Mn_i in the band gap is the one that dominates recombination and therefore eventually reduces solar cell efficiency. The defect parameters of interstitial manganese have been determined using lifetime spectroscopy.

5 CONCLUSION

In this study, the manganese-related, lifetime-reducing defect centre in float-zone grown boron-doped silicon was investigated and analysed in depth. The energy level and majority carrier capture cross section of manganese-boron pairs (MnB) have been determined to $E_t - E_V = 0.54 \pm 0.02$ eV and $\sigma_p = 3.5\times10^{-13}$ cm^2 by deep-level transient spectroscopy at low temperatures. Subsequently, these MnB pairs have been dissociated optically and thermally. Furthermore, the recombination-dominating defect level of interstitial manganese in silicon could be determined to $E_C - E_t = 0.46 \pm 0.04$ eV and $\sigma_n = (9 \pm 7)\sigma_p$ by means of temperature-dependent lifetime spectroscopy.

ACKNOWLEDGEMENTS

One of the authors (T.R.) gratefully acknowledges a scholarship of the German Federal Environmental Foundation (Deutsche Bundesstiftung Umwelt), another one (D.M.) is supported by an Australian Council QEII Fellowship. The authors are also grateful to R. Elliman, C. Jagadish and H. Tan of ANU for access to the ion implantation and PECVD equipment.

REFERENCES

[1] A.A. Istratov, H. Hieslmair, and E.R. Weber, Appl. Phys. A (Materials Science & Processing) A69 (1999) 13.
[2] D.V. Lang, J. Appl. Phys. 45 (1974) 3023.
[3] S. Rein, T. Rehrl, W. Warta, and S.W. Glunz, J. Appl. Phys. 91 (2002) 2059.
[4] K. Graff, Metal Impurities in Silicon-Device Fabrication, 2nd ed., Springer, Berlin (1999).
[5] G.W. Ludwig and H.H. Woodbury, Phys. Rev. Lett. 5 (1960) 98.
[6] G.H. Ludwig and H.H. Woodbury, Solid State Physics 13 (1962) 223.
[7] R.O. Carlson, Phys. Rev. 104 (1956) 937.
[8] H. Nakashima and K. Hashimoto, J. Appl. Phys. 69 (1991) 1440.
[9] H. Lemke, phys. stat. sol. (a) 64 (1981) 549.
[10] H. Lemke, phys. stat. sol. (a) 71 (1982) K215.
[11] M. Haider, H. Sitter, R. Czaputa, H. Feichtinger *et al.*, J. Appl. Phys. 62 (1987) 3785.
[12] H. Lemke, phys. stat. sol. (a) 83 (1984) 637.
[13] R. Czaputa, H. Feichtinger, J. Oswald, H. Sitter *et al.*, Phys. Rev. Lett. 55 (1985) 758.
[14] D. Macdonald, P. Rosenits, and P.N.K. Deenapanray, Semicond. Sci. Technol. 22 (2007) 163.
[15] D. Macdonald, P.N.K. Deenapanray, and S. Diez, J. Appl. Phys. 96 (2004) 3687.
[16] D. Gilles, W. Schröter, and W. Bergholz, Phys. Rev. B 41 (1990) 5770.
[17] R.A. Sinton and A. Cuevas, Appl. Phys. Lett. 69 (1996) 2510.